



A 2-oxoglutarate-dependent dioxygenase converts dihydrofuran to furan in *Salvia* diterpenoids

Jiao-Jiao Song ^{1,2,†}, Xin Fang,^{3,†} Chen-Yi Li,⁴ Yan Jiang,^{1,5} Jian-Xu Li,⁴ Sheng Wu ^{1,6}, Juan Guo ⁷, Yan Liu,^{1,2} Hang Fan ¹, Yan-Bo Huang,¹ Yu-Kun Wei,¹ Yu Kong,¹ Qing Zhao,¹ Jing-Jing Xu,¹ Yong-Hong Hu ¹, Xiao-Ya Chen,^{1,4} and Lei Yang ^{1,*,#}

- 1 Shanghai Key Laboratory of Plant Functional Genomics and Resources, Shanghai Chenshan Botanical Garden, Shanghai 201602, China
- 2 University of Chinese Academy of Sciences, Beijing 100049, China
- 3 State Key Laboratory of Phytochemistry and Plant Resources in West China, Kunming Institute of Botany, Chinese Academy of Sciences, Kunming 650201, China
- 4 State Key Laboratory of Plant Molecular Genetics, CAS Center for Excellence in Molecular Plant Sciences/Shanghai Institute of Plant Physiology and Ecology, Chinese Academy of Sciences, Shanghai 200032, China
- 5 School of Life Sciences, Shanghai Normal University, Shanghai 200234, China
- 6 Department of Chemical and Environmental Engineering, University of California, Riverside, California 92521, USA
- 7 State Key Laboratory of Dao-di Herbs, National Resource Center for Chinese Materia Medica, China Academy of Chinese Medical Sciences, Beijing 100700, China

*Author for communication: leiyang@cemps.ac.cn

†These authors contributed equally (J.-J.S., X.F.).

#Senior author

L.Y. and X.-Y.C. designed and managed the project. J.-J.S., Y.L., and L.Y. isolated the genes and characterized the enzyme, X.F., C.-Y.L., S.W., Q.Z., and J.G. helped in the biosynthetic pathway analysis. J.-X.L., H.F., and J.-J.X. performed bioinformatics analysis. Y.-B.H. and Y.-K.W. collected and cultured plants. Y.K. assisted with LC-MS analysis. X.-Y.C. and Y.-H.H. analyzed and interpreted the data. L.Y., X.F., and X.-Y.C. wrote the manuscript.

The author responsible for distribution of materials integral to the findings presented in this article in accordance with the policy described in the Instructions for Authors (<https://academic.oup.com/plphys/pages/general-instructions>) is: Lei Yang, leiyang@cemps.ac.cn

Abstract

Tanshinone IIA (TIIA), a diterpene quinone with a furan ring, is a bioactive compound found in the medicinal herb red-root sage (*Salvia miltiorrhiza* Bunge), in which both furan and dihydrofuran analogs are present in abundance. Progress has been made recently in elucidating the tanshinone biosynthetic pathway, including heterocyclization of the dihydrofuran D-ring by cytochrome P450s; however, dehydrogenation of dihydrofuran to furan, a key step of furan ring formation, remains uncharacterized. Here, by differential transcriptome mining, we identified six 2-oxoglutarate-dependent dioxygenase (2-ODD) genes whose expressions corresponded to tanshinone biosynthesis. We showed that Sm2-ODD14 acts as a dehydrogenase catalyzing the furan ring aromatization. In vitro Sm2-ODD14 converted cryptotanshinone to TIIA and thus was designated TIIA synthase (SmTIIAS). Furthermore, SmTIIAS showed a strict substrate specificity, and repression of SmTIIAS expression in hairy root by RNAi led to increased accumulation of total dihydrofuran-tanshinones and decreased production of furan-tanshinones. We conclude that SmTIIAS controls the metabolite flux from dihydrofuran- to furan-tanshinones, which influences medicinal properties of *S. miltiorrhiza*.

Introduction

Plants of the family Lamiaceae produce a rich array of diterpenoids of varied skeletons (Johnson et al., 2019). *Salvia miltiorrhiza* Bunge, a medicinal species known as Danshen or red sage in China, accumulates in roots a group of abietane-type *nor*-diterpenes, collectively named tanshinones (Dong et al., 2011). To date, a total of 81 tanshinones were identified, which show therapeutically relevant biological activities including antibiotic, anti-inflammatory, and antioxidant properties (Wang et al., 2007). Due to their structural uniqueness and medicinal interests, the biosynthesis of tanshinones has been investigated intensively in last two decades (Figure 1). The diterpene synthases *S. miltiorrhiza* copalyl diphosphate synthase 1 and *S. miltiorrhiza* kaurene synthase-like 1 produce the tricyclic miltiradiene (Gao et al., 2009), then the CYP76AH subfamily enzymes hydroxylate and aromatize the C-ring, followed by C20 hydroxylation by CYP76AK1 (Guo et al., 2013, 2016). Very recently, two CYP71D enzymes (CYP71D375 and CYP71D373) were shown to catalyze the D-ring formation through C16 hydroxylation and 14,16-ether (hetero) cyclization, leading to the formation of dihydrofuran-tanshinones from their respective precursors (Ma et al., 2021).

Among the tanshinones in *S. miltiorrhiza*, tanshinone IIA (TIIA) is considered the major active ingredient (Fang et al., 2021). In 3T3-L1 cells and zebrafish TIIA inhibited lipid accumulation (Park et al., 2017), and the derivate sodium TIIA silate is used in China for alleviating cardiovascular and coronary heart diseases (Li et al., 2020b). Both T I and TIIA, differing in A-ring aromatization, are typical tetracyclic tanshinones featuring an *ortho*-quinone C-ring and a furan D-ring (Figure 1), while cryptotanshinone (CT) and 15,16-dihydrotanshinone I (DTI) with dihydrofuran ring were believed to be their precursors, respectively (Ma et al., 2021). However, till now, aromatization of the D-ring to a furan in tanshinone biosynthesis remains uncharacterized.

Furan moieties occur in a wide variety of natural products, including many pharmaceuticals. Despite their importance, our understanding of the furan ring desaturation mechanism remains rudimentary. CYP71AJ1 and CYP71AJ4 in plants of the Apiaceae family catalyze the formation of linear and angular furanocoumarins, respectively, through concomitant carbon-chain cleavage and acetone releasing which, however, do not involve a separate desaturation step during furan formation (Larbat et al., 2007, 2009). In the biosynthesis of flavonoids, flavonol synthase and flavone synthase I, both belonging to the 2-oxoglutarate-dependent dioxygenase (2-ODD) family, catalyze C2–C3 desaturation to form the central pyran ring (Turnbull et al., 2004; Cheng et al., 2014). To date, the enzymes responsible for converting dihydrofuran or tetrahydrofuran to furan have not been identified.

In plants, the 2-ODD or 2-OGD superfamily comprises the second largest enzyme family besides the cytochrome P450s (CYPs). Based on similarity of the amino acid sequences, the plant 2-ODD family could be divided into DOXA, DOXB,

and DOXC classes (Kawai et al., 2014). DOXA and DOXB function in nucleotide and protein modification, respectively; while DOXC class is involved in secondary metabolism of various phytochemicals including glucosinolates, flavonoids, and alkaloids (Araujo et al., 2014), by which the plant defend against biotic stresses (Ge et al., 2021). 2-ODD members facilitate numerous oxidative reactions, including hydroxylation, desaturation, demethylation, halogenation, epoxidation, and ring formation (Islam et al., 2018). Genome-wide analysis of 2-ODD superfamily has been reported in *S. miltiorrhiza* and, based on RNAi data obtained from hairy roots, 2OGD5 was found to affect the accumulation of CT, TIIA, and miltirone (Xu and Song, 2017), but the biochemical evidence was lacking.

Here, we characterize a 2-ODD protein from *S. miltiorrhiza*, which catalyzes the desaturation of the dihydrofuran ring in CT and isoCT (iCT), and was designated *S. miltiorrhiza* TIIA synthase (SmTIIAS). In addition, among the 2-ODD candidates screened, SmTIIAS is the only active dihydrofuran desaturase and exhibits high substrate selectivity. We propose that SmTIIAS represents an example of furan synthase in general, in addition to be a key enzyme responsible for channeling dihydrofuran-tanshinones to the furan products.

Results

Mining 2-ODDs upregulated in root

The biosynthesis and accumulation of secondary metabolites tend to be tissue-specific, and the enzymes involved are expected to share a similar gene expression pattern (Murata et al., 2008; Beaudoin and Facchini, 2014). Although trace amounts of tanshinones can be detected in the aerial tissues of *S. miltiorrhiza*, these diterpenoids are primarily synthesized and stored in root (Li et al., 2008a; Yang et al., 2013). To mine the candidate enzymes responsible for the desaturation of the dihydrofuran ring in tanshinones, we generated transcriptomes of root and leaf tissues of this species, respectively. The RNA-seq produced 112,846 unigenes, of which 44.41% were annotated in SWISSPROT database (Supplemental Table S1). After differential expression analysis (fold change > 2), we obtained 12,048 genes which were upregulated in root compared to leaf (Figure 2A), among which a total of 18 genes were annotated by scanning DIOX_N and 2-oxoglutaric acid (2OG)-Fell_Oxy domains to encode 2-ODDs, namely Sm2-ODD1 to 18 (Figure 2B; Supplemental Table S2). Except for Sm2-ODD11 and Sm2-ODD16, other 16 Sm2-ODDs have homologs (amino acid sequence identity ranged from 96.26% to 100%) to those previously reported by Xu and Song (2017) (Supplemental Table S2); however, none of Sm2-ODDs showed high identity to 2OGD5 (Xu and Song, 2017).

Another species of the genus, *Salvia substolonifera*, has a much lower relative content of tanshinones, such as CT, TIIA, tanshinone I, and miltirone, in its root (Figure 2C; Supplemental Figure S1), which provided a good reference to select the genes of the tanshinone pathway. We thus

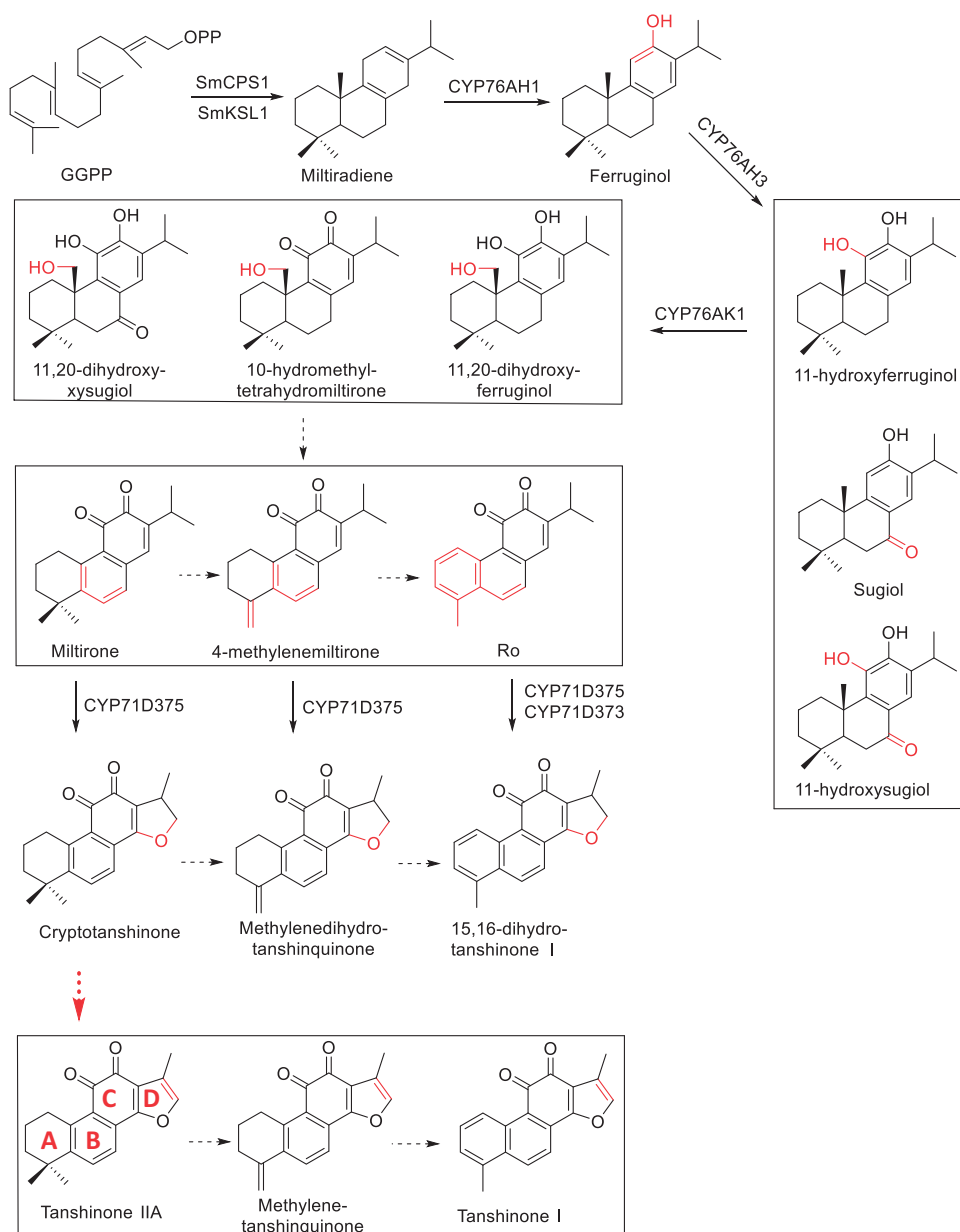


Figure 1 The biosynthetic pathway of tanshinones in *S. miltiorrhiza*. Solid arrows denote the known steps, dashed arrows denote the hypothetical steps, and the red arrow indicates the step will be elucidated in present study. The promiscuity of identified CYPs suggests a metabolic grid architecture for diterpenoid biosynthesis.

compared the relative transcript levels of the 18 2-ODDs in roots of these two *Salvia* species. The FPKM (Fragments Per Kilobase of exon model per Million mapped fragments) values from the Illumina-generated RNA-seq data narrowed the 18 2-ODD genes down to six, including *Sm2-ODD7*, *Sm2-ODD8*, *Sm2-ODD14*, *Sm2-ODD16*, *Sm2-ODD17*, and *Sm2-ODD18*, whose transcript levels were clearly higher in *S. miltiorrhiza* than in *S. substolonifera* (Figure 2D), suggesting that they could serve as oxidative enzymes in the biosynthesis of TIIA, tanshinone I, or structurally related diterpenoids.

Functional characterization of Sm2-ODD14

The six 2-ODDs, namely *Sm2-ODD7*, *Sm2-ODD8*, *Sm2-ODD14*, *Sm2-ODD16*, *Sm2-ODD17*, and *Sm2-ODD18*, were

then expressed in *Escherichia coli*. In subsequent in vitro assays, only the recombinant protein of *Sm2-ODD14* was active toward CT and converted it into a single product (Figure 3A), which was determined to be TIIA by comparison to the authentic standard in Q Exactive (QE) plus mass analysis (Figure 3B); consequently, the enzyme was designated *SmTIIAS*, because other products such as methylene-tanshinquinone and tanshinone I derived from TIIA were not detected in the enzymatic assay. To define the substrate spectrum of *Sm2-ODD14*, several structural analogs of CT, including methylenedihydro-tanshinquinone, DTI, iCT, tetrahydro-tanshinone I, and 1,2-didehydrocryptotanshinone, were tested. *Sm2-ODD14* was found to be able to convert iCT to isotanshinone IIA (iTIIA) (Figure 3, C and D), but inactive

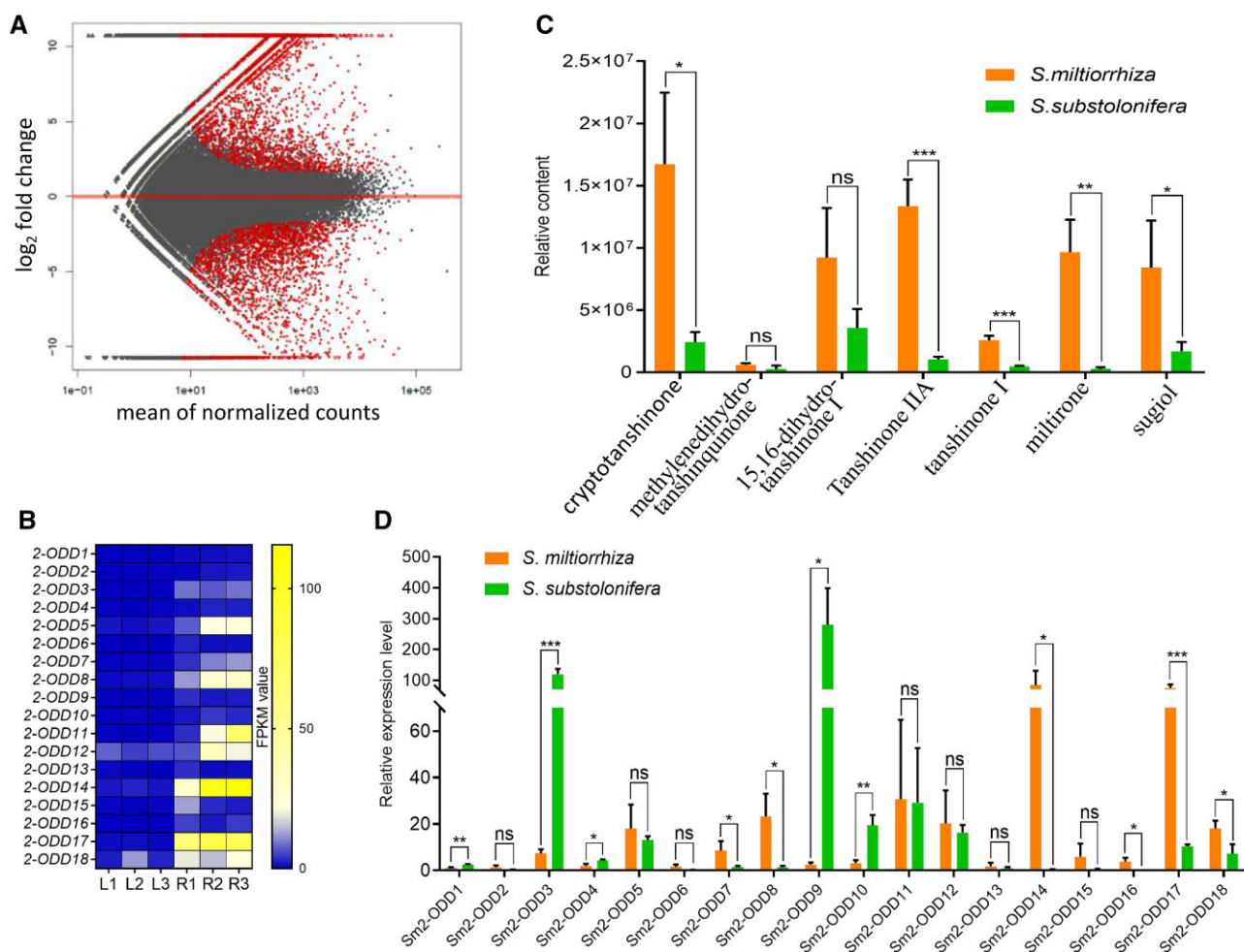


Figure 2 The mining of candidate 2-ODDs involved in the tanshinone biosynthetic pathway in *S. miltiorrhiza*. A, Differentially expressed genes in leaf and root, the up- and down-regulated genes are indicated by red spots. B, The transcript levels of 18 2-ODD genes by FPKM in *S. miltiorrhiza* root (R) and leaf (L) transcriptomes. C, Accumulation of tanshinones in root of *S. miltiorrhiza* and *S. substolonifera*. D, Expression levels of the 18 candidate 2-ODDs by FPKM in roots of *S. miltiorrhiza* and *S. substolonifera*. For (C) and (D), Data are means \pm sd (Standard Deviation) of three biological replicates. Statistical analysis was performed with Student's *t* test. **P* < 0.05; ***P* < 0.01, ****P* < 0.001, and ns indicates no significance.

to other compounds (Supplemental Figure S2). Structurally, CT and iCT are different from other analogs in sharing a saturated A-ring with two methyl groups, which may be the key feature recognized by Sm2-ODD14. In conclusion, Sm2-ODD14 acted as a desaturase and introduced a double bond between C15 and C16 to complete the furan ring formation.

To optimize the reaction conditions, the activities of recombinant proteins were assessed with CT as substrate at different temperatures (20°C, 28°C, and 37°C) and pH values (6.5 and 7.4), and the optimal condition was fixed to be at 20°C and pH 6.5 (Supplemental Figure S3). To test the effects of cofactors on enzymatic activity, we first omitted 2OG in the assay, which abolished the SmTIIAS activity. In addition, although not indispensable, the cofactors L-ascorbic acid (ASC) and Fe²⁺ facilitated the catalysis (Supplemental Figure S4a), likely through promoting the enzyme–substrate interaction. Kinetic analysis with CT and iCT in the presence of 2OG, ASC, and Fe²⁺ showed that

the *K_m* values of SmTIIAS were 67.71 ± 7.30 and $29.71 \pm 10.51 \mu\text{M}$, the estimated *k_{cat}* values were 0.60 ± 0.03 and $0.27 \pm 0.09 \text{ s}^{-1}$, and the *k_{cat}/K_m* were $8,843.45 \pm 546.65 \text{ s}^{-1}\text{M}^{-1}$ and $9,200.85 \pm 353.52 \text{ s}^{-1}\text{M}^{-1}$, respectively (Supplemental Figure S4, b and c). Although the enzyme showed higher affinity toward iCT, considering TIIA being much more abundant than iTIIA in *S. miltiorrhiza*, the function of SmTIIAS *in planta* is mainly catalyzing the conversion of CT to TIIA.

The tissue-specific expression pattern of SmTIIAS were analyzed by using reverse transcription quantitative PCR (RT-qPCR) which showed the highest relative expression level in root and much lower levels in aerial tissues, especially in stem and inflorescence the expression levels were nearly undetectable (Figure 3E). This result is in agreement of the root-specific accumulation of tanshinones (Li et al., 2008a; Yang et al., 2013). Furthermore, the enhancement of the accumulation of tanshinones was reported to be triggered by treatment of several phytohormones including methyl

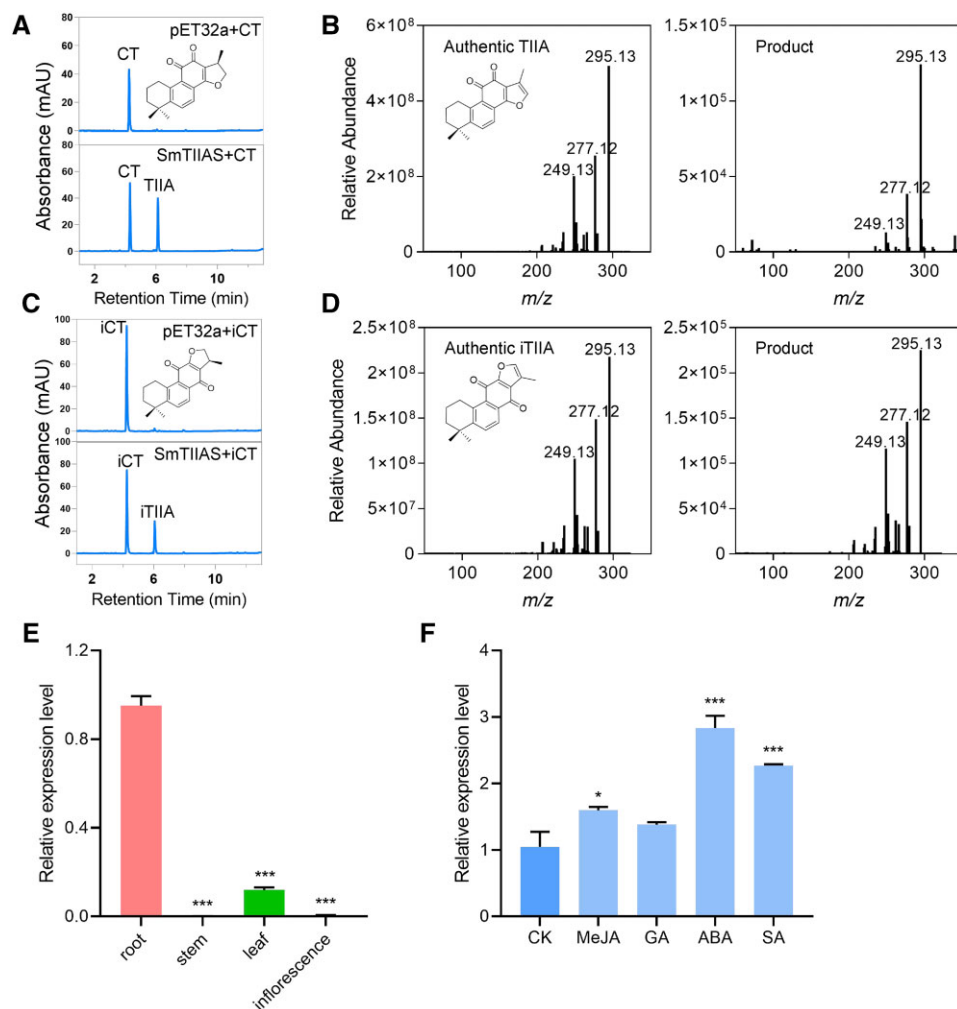


Figure 3 Characterization of *SmTIIAS* by *in vitro* assay and its relative expression. A, UPLC profile of the product generated by *SmTIIAS* with CT as substrate. B, Authentic standard of TIIA and the *SmTIIAS* product, detected by QE. C, UPLC profile of the product of *SmTIIAS* incubated with iCT as substrate. D, Authentic standard of iTIIA and the *SmTIIAS* product, detected by QE. The recombinant protein of *SmTIIAS* were incubated with the indicated substrate at 20°C, for 7 min. E, Relative expression of *SmTIIAS* in different tissues. F, Relative expression of *SmTIIAS* after different phytohormone treatments, including MeJA, SA, ABA, GA, and with DMSO solution (5%) as control (CK). For (E) and (F), data are means \pm SD of three biological replicates. Statistical analysis was performed with Student's *t* test.

jasmonate (MeJA), salicylic acid (SA), abscisic acid (ABA), and gibberellic acid (GA) (Pei et al., 2018). Accordingly, the expression levels of *SmTIIAS* increased after treatment of the hairy roots culture of *S. miltiorrhiza* by ABA and SA and at a very limited level by MeJA (Figure 3F). These results further confirmed the function of *SmTIIAS* in tanshinones biosynthesis.

Silencing *SmTIIAS* in hairy root reduced the formation of furan-tanshinones

To prove the function of *SmTIIAS* *in vivo*, we repressed the *SmTIIAS* expression in *S. miltiorrhiza* hairy roots by RNA interference (RNAi), using a *SmTIIAS*-specific region of 395 bp with no or low sequence identity to other 17 2-ODD sequences. Three RNAi hairy root lines (RNAi-L1, RNAi-L3, and RNAi-L7) were selected, in which the *SmTIIAS* transcript level was decreased to 30%–50% of the WT level

(Figure 4A). Analysis of the metabolites by UPLC (Ultra Performance Liquid Chromatography) showed that the level of TIIA was decreased from 0.66 mg g⁻¹ DW (dry weight) in the control to 0.08, 0.09, and 0.16 mg g⁻¹ DW in the three RNAi hairy root lines, respectively; the *SmTIIAS* substrate CT, in contrast, was over-accumulated in the RNAi hairy roots (Figure 4, B and C). Notably, the contents of methylenedihydro-tanshinquinone and DTI also increased in the RNAi roots, while the tanshinone I level was reduced (Figure 4C; Supplemental Figure S5). Some tanshinones contents, such as methylenetanshinquinone, TIIB, and tanshin-diol A, were too low to be quantified both in the WT and the RNAi hairy root lines. Since *SmTIIAS* could not accept methylenedihydro-tanshinquinone or DTI as substrates, knocking-down the *SmTIIAS* expression could not directly result in accumulation of these dihydrofuran-tanshinones. A more likely scenario is that the A-ring decorating enzymes

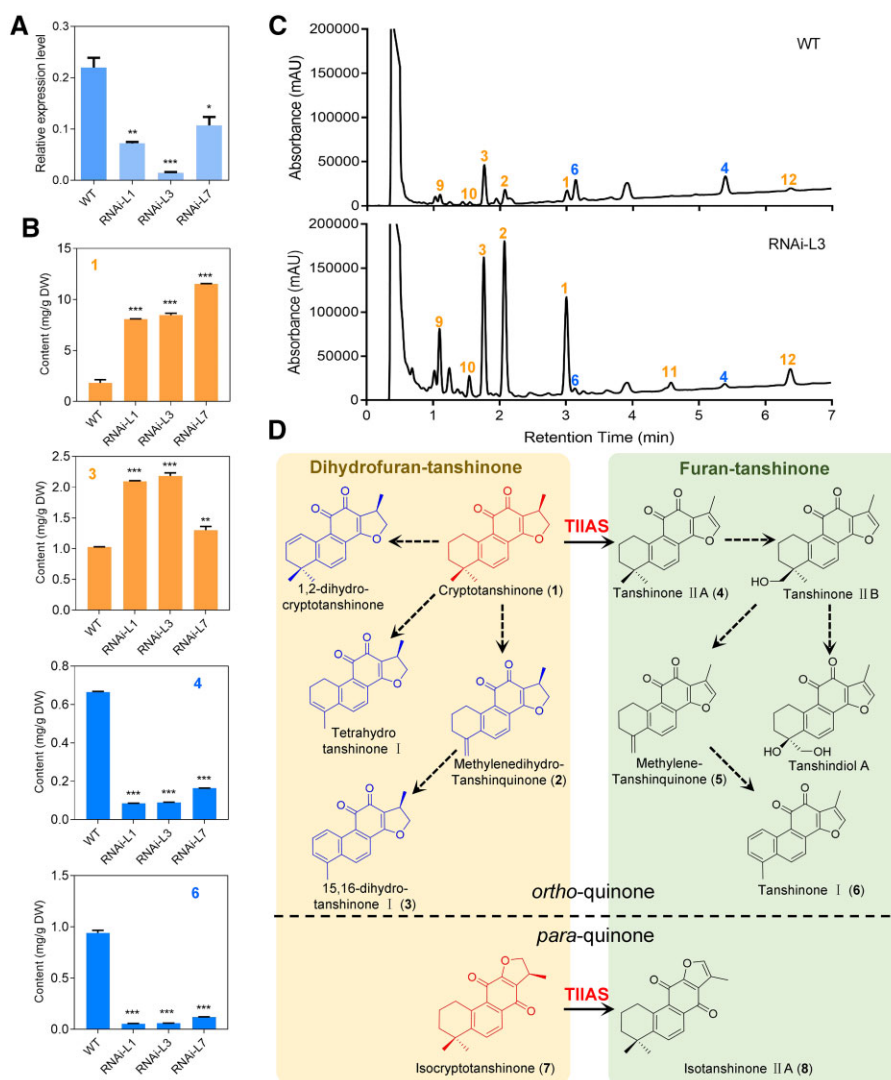


Figure 4 The effects of *SmTIIAS* silencing by RNAi on the accumulation of tanshinones. A, Relative expression of *SmTIIAS* in the RNAi hairy root lines detected by RT-qPCR (reverse transcription quantitative PCR). B, Contents of four tanshinones in the RNAi hairy roots (numbers shown in the panels correspond with the numbered compounds in (D)). Data are means \pm SD of three biological replicates. Statistical analysis was performed with Student's *t* test. C, UPLC comparison of the WT and the RNAi hairy roots, line 3 (RNAi-L3). The mass spectra of the compounds were given in [Supplementary Figure S5](#). Orange color and blue color indicate the increased and decreased content of compounds in the RNAi line, respectively. D, The catalytic role of *SmTIIAS* in converting dihydrofuran-tanshinones to furan-tanshinones. The structures in red, but not those in blue, were accepted by *SmTIIAS*. Peaks in the total ion chromatograms of (C) are numbered and assigned to corresponding structures (with identical numbers) in (D) while peaks marked with 9–12 could not be assigned structures, and the corresponding mass spectra were given in [Supplemental Figure S5](#).

do not distinguish between the dihydrofuran and furan D-ring, and the conversion from CT to TIIA catalyzed by *SmTIIAS* is the major path to the formation of furan-tanshinones, and the decreased transcript level of *SmTIIAS* impeded the flux toward furan-tanshinones that resulted in accumulation of dihydrofuran-tanshinones, including CT, methylenedihydro-tanshinquinone and DTI (Figure 4D).

Lineage specificity of TIIAs in *Salvia* species

Salvia, the largest genus within Lamiaceae, is widely distributed throughout tropical and temperate regions of the world. Tanshinones are distributed in *Salvia* species in Himalayan and East Asia (Li et al., 2008b; Hu et al., 2018).

Assay of *SmTIIAS* orthologous proteins from three other tanshinone-producing *Salvia* species distributed in East Asia including *S. meiliensis*, *S. bowleyana*, and *S. trijuga* showed that they all have the desaturation activity against the dihydrofuran ring in CT (Figure 5A; Supplemental Figure S6).

2-ODDs of the DOXC class are classified into 57 phylogenetic clades (DOXC1-57) (Kawai et al., 2014). To discern the evolution of TIIAs from ancestral 2-ODDs, we compared the TIIAs with other DOXC 2-ODD proteins which have been characterized experimentally (Kawai et al., 2014; Caarls et al., 2017; Kakizaki et al., 2017; Nakayasu et al., 2017; Li et al., 2020a). In the phylogenetic tree constructed the *SmTIIAS* and orthologous sequences from *Salvia* species

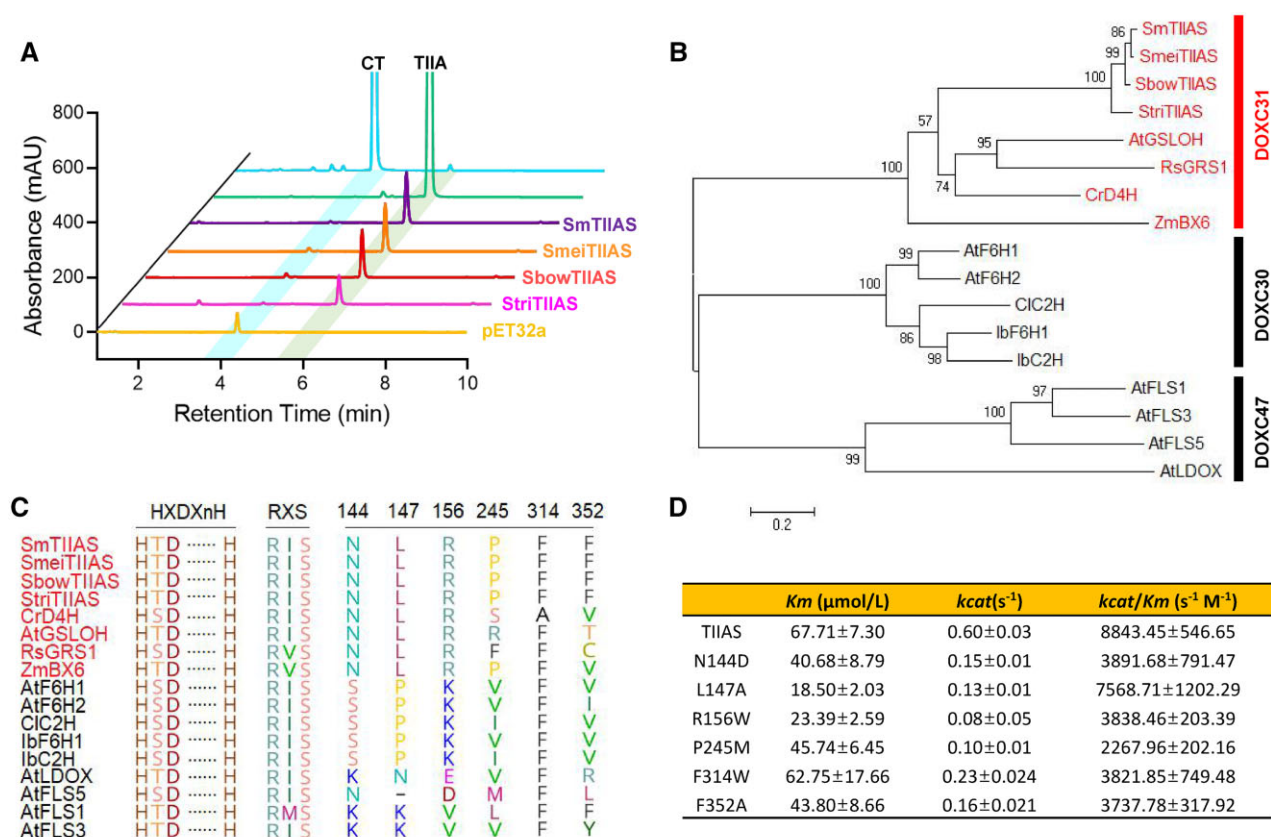


Figure 5 Evolution of TIIASs. (A) Identification of TIIASs from *Salvia* species. CT and TIIA are the substrate and product, respectively. B Phylogenetic tree of TIIASs with reported 2-ODD activities. The phylogenetic tree was constructed by the maximum likelihood method, and the branches indicate bootstrap values calculated by the 1,000 permutation test. Scale bar indicates 0.2 substitutions per position in the sequence. The classification was according to Kawai et al. (2014) and red fonts indicate the DOXC D4H/BX6 clade. C, Multiple sequence alignment of TIIASs and other 2-ODD proteins with the conserved and specified domains highlighted. D, Steady-state kinetic parameters of SmTIIAS and its substitution mutants by in vitro enzymatic assays. Assays were carried out in triplicate. Data represent the mean \pm SE of values.

were classified into the DOXC31 (namely D4H/BX6) clade (Figure 5B; Supplemental Figure S7), which in *Arabidopsis* (*Arabidopsis thaliana*) is the largest group (Kawai et al., 2014). Accordingly, the D4H/BX6 clade sequences were selected for multiple alignments. As a canonical 2-ODD, the 373-aa-long peptide of SmTIIAS not only contains the C-terminal 2OG-FeII_OXY domain with the dominate feature of the 2-HIS-1-carboxylate facial triad (residues His 242, Asp 244 and His 301) involved in iron binding, but also the key residues (Arg 308 and Ser 310) involved in the 2OG co-substrate binding. From the alignment, the residues Asn144, Leu147, and Arg156 are conserved in the D4H/BX6 clade, whereas Pro245 and Phe352 are specific to TIIASs (Figure 5C). Data from substitution mutants supported the predicted residues to bind the substrate CT (Figure 5D).

Discussion

The 2-ODD superfamily enzymes catalyze various oxidative reactions including hydroxylation, demethylation, halogenation, desaturation, epoxidation, and ring formation (Islam et al., 2018). Furan moiety is present in several classes of natural products, such as furanoflavonoids, furanocoumarins,

and terpenoids. Being a nonpolar aromatic component, furan derivatives have a unique place in the field of medicinal chemistry. For examples, rotundifuran, a labdane-type diterpene from the fruit of Beach vitex (*Vitex rotundifolia*), showed inhibitory effect on human myeloid leukemia HL-60 cell proliferation (Ko et al., 2001), and the furan-coumarin conjugate geiparvarin from leaves of Australian Willow (*Geijera parviflora*) has antitumor properties (Viola et al., 2004). Our finding reported herein provides a previously unknown mechanism for aromatization of furan structures.

The 2-ODDs are believed to originate from a common ancestor before land plant emerged, then underwent species-specific evolution under varied environments (Ge et al., 2021). Phylogenetic analysis showed that TIIASs belong to the DOXC D4H/BX6 clade, which is the largest DOXC group in *S. miltiorrhiza* and may participate in the tanshinone biosynthesis based on genome-wide strategy (Xu and Song, 2017). This clade contains functionally diverse 2-ODDs among which most function as hydroxylase. For instance, ZmBX6 from maize (*Zea mays*), CrD4H from rosy periwinkle (*Catharanthus roseus*), and *Arabidopsis* AtGSLOH catalyze the hydroxylation of DIBOA glucoside, desacetoxvindoline (monoterpenoid indole alkaloids), and 3-butenyl

glucosinolate, respectively (Vazquez-Flota et al., 1997; Hansen et al., 2008; Jonczyk et al., 2008), whereas RsGRS1 from radish (*Raphanus sativus*) is responsible for the desaturation of the side chain of glucoerucin (Kakizaki et al. 2017). The phylogenetic analyses reveal that TIIASs evolved in *Salvia* species distributed in the Himalayan and East Asian region, which served as a driving force of the furan-tanshinones innovation.

Both 2-ODDs and CYPs oxidize plant metabolites to create structural diversity. However, 2-ODDs invariably use hydrophilic substrates, often modified by CYPs, partially due to the cytosolic nature of the former (Kakizaki et al., 2017). Thus, it is suggested that 2-ODDs diversified following expansion of CYPs (Hedden and Thomas, 2012; Farrow and Facchini, 2014), which is also the case in *Salvia*. Notably, the CYPs in the *Salvia* diterpenoid pathway, such as CYP76AH3, CYP76AK1, and CYP71D375, generally show catalytic promiscuity (Figure 1), which create a metabolic grid for tanshinones biosynthesis. In contrast, SmTIIAS is a rather specific enzyme that could not recognize the dihydrofuran-tanshinones with a modified A-ring (Figure 4D). Considering the promiscuity of the CYPs that act upstream to SmTIIAS, the downstream CYPs may be similarly less stringent, and the metabolic grid also exists downstream of SmTIIAS. Consistent with this hypothesis, silencing of SmTIIAS shifted the diterpenoid flux toward the accumulation of not only CT but also other dihydrofuran-tanshinones (Figure 4, B and C). Our data suggest that SmTIIAS functions at the bottleneck step to control the production of furan-tanshinones. Thus, a single enzyme SmTIIAS extends the structural diversity of tanshinones in that quite a lot of tanshinones have either furan or dihydrofuran D-ring. Interestingly, in the genus *Solanum*, a short-chain dehydrogenase/reductase was found to be responsible for divergence of saturated/unsaturated steroidal glycoalkaloids (SGAs), two major group of SGAs (Sonawane et al., 2018). This coincidence implies presence or absence of double bonds in core scaffold of natural products may be a major source of structural diversity and the corresponding enzymes act on a key branch point in the biosynthesis pathways. Besides, except for SmTIIAS identified here, there may be other 2-ODDs involved in tanshinone biosynthesis, such as 2OGD5, RNAi knockdown of which affects the accumulation of CT, TIIA, and miltirone (Xu and Song, 2017).

Tanshinones are a group of abietane-type *nor*-diterpenes that present in plant in a mixture form. Biosynthetic studies revealed that these compounds are often biosynthetic intermediates from miltiradiene to tanshinone I, including CT, methylenedihydro-tanshinquinone, DTI, and TIIA. Thus, the biosynthesis of tanshinones is different from such pathways that accumulate one main end product such as gossypol in cotton (*Gossypium* spp.) or artemisinin in sweet Annie (*Artemisia annua*), in which the route is linear and the enzymes are more substrate-specific (Tian et al., 2018; Huang et al., 2021). Silencing of biosynthetic enzymes of these types led to reduction of end product and

accumulation of corresponding intermediates that in some cases could be harmful to the host (Tian et al., 2019). Meanwhile, the biosynthesis of tanshinones involves metabolic grid and promiscuous enzymes, which release several intermediates with different pharmacological activities.

Among the mixture of diterpenoids in *S. miltiorrhiza*, TIIA is the most abundant lipophilic constituent, and the furano-*o*-quinone is the core moiety unique to this group of *nor*-diterpenoids (Zhang et al., 2008; Ma et al., 2021). The presence of D-ring was reported to contribute substantially to anti-cancer activity of the tanshinones (Wang et al., 2014), and the furan oxygen plays a key role due to its involvement in the minor groove-binding of DNA (Zhang et al., 2008). Identification of the enzyme catalyzing the hetero-aromatization of dihydrofuran-tanshinones paves the way to design potential pharmaceutical resources.

Conclusion

Here we have demonstrated that one 2-ODD gene encodes SmTIIAS *in vitro* and *in planta*. SmTIIAS is the first enzyme characterized to dehydrogenate the dihydrofuran ring to a furan, a key step in furan ring formation. It shows a strict substrate specificity to CT and iCT and is a key enzyme responsible for channeling dihydrofuran- to the furan-tanshinones which, including TIIA, are considered the most effective ingredient in *S. miltiorrhiza*. Our finding is important not only to medicinal plants but also to plant secondary metabolism.

Materials and methods

Plant materials and chemicals

Plants of *Salvia* species were grown in nursery in Shanghai Chenshan Botanical Garden. Roots and leaves of the 1-year-old plants were sampled, three plants as triplicates, and desiccated in lyophilizer (Thermo) for subsequent analysis.

The standard compounds CT, DTI, TIIA, and tanshinone I were purchased from Sigma-Aldrich Corp. (St Louis, USA), tetrahydro-tanshinone I, 1,2-didehydrocryptotanshinone, iCT, and iTIIA were purchased from Shanghai Yuanye Bio-Technology CO. Ltd., and methylenedihydro-tanshinquinone was kindly provided by Prof. Juan Guo. MeJA was purchased from Sigma-Aldrich Corp., SA, ABA, and GA were purchased from Sangon Biotech (Shanghai) Co. Ltd.

RNA sequencing and candidate genes mining

The root and leaf RNA samples of *Salvia* species were profiled by HiSeq X Ten (Illumina San Diego, CA, USA) platform with paired-end method in which each sample contained three replicates, and the sequencing and data analysis were performed by Shanghai Oebiotech CO. Ltd. Annotation information was listed in Supplementary Table S1. Taking a significance level of $P < 0.05$ and Log2 fold-change > 2 as a threshold, we obtained 12,048 upregulated unigenes in root compared with leaf tissue of *S. miltiorrhiza*.

Based on the upregulated unigenes, *Arabidopsis* (*A. thaliana*) 2-ODD proteins (<https://www.arabidopsis.org/>) were used to local tblastn against the *S. miltiorrhiza* unigenes at a cut-off *e*-values of e^{-10} . Then the newest HMM (hidden Markov model) profile of 2-ODD domain (PF03171 and PF14226) from Pfam database (<http://pfam.xfam.org/>) was used to search the Sm2-ODDs in protein database of *S. miltiorrhiza* on HMMER program (<https://www.ebi.ac.uk/Tools/hmmer/>) with a cut-off *e*-value of 10^{-4} , which led to 18 common 2-ODDs candidate genes as listed in [Supplementary Table S2](#).

Sequence alignment and phylogenetic analysis

The sequences for sequence alignment and phylogenetic analysis were obtained from National Center for Biotechnology Information (NCBI) database. Sequences alignments were performed using the MUSCLE algorithm in MEGA version 6 software package (Tamura et al., 2013). Phylogenetic tree was constructed by using the maximum-likelihood method on the LG model, with Gamma distributed rate variation among sites and a proportion of Invariant sites (G + I). Bootstrap statistics were calculated using 1,000 replicates. All phylogenetic analyses were conducted in MEGA version 6. The accession numbers of the proteins in the phylogenetic tree are listed in [Supplemental Table S3](#).

cDNA cloning and heterogeneous expression

The RNA of *S. miltiorrhiza* root was extracted using cetyltrimethylammonium bromide (CTAB) solution (2% [w/v] CTAB, 2% [w/v] PVP, 100 mM Tris-HCl, 25 mM EDTA, 2M NaCl, and 2% β -mercaptoethanol) (Fang et al., 2017). Taking 1 μ g of RNA of sample above performed reverse transcript following instruction of cDNA Synthesis Kit (TOYOBO, Osaka, Japan). The primers ([Supplemental Table S4](#)) were designed for amplifying 2-ODD sequences using KOD DNA polymerase (TOYOBO).

After digesting by Bam HI and Not I (Thermo Scientific, Waltham, MA, USA), the PCR amplicon of coding sequence was cloned into vector pET32a, and the pET32a-2ODD vectors were introduced into *E. coli* Rosetta 2 (DE3). The protein expression was induced by β -D-1-thiogalactopyranoside. After harvesting the cultures, crude protein lysate was centrifuged and purified with affinity chromatography with nickel nitrilotriacetic acid resin (Thermo Scientific), and the protein concentration was determined with bovine serum albumin standard.

Enzyme activity assays

In vitro activity assay was performed in a 200- μ L reaction system consisting of 200 mM 2-(N-morpholino) ethanesulfonic acid (MES, pH 6.5), 200 μ M 2OG, 200 μ M L-ASC, 100 μ M FeSO₄, 200 μ M adenosine triphosphate, the substrate (3.75–150 μ M) and 100 μ g purified recombinant protein. After shaking with sufficient air at 20°C for 7 min, the reaction was stopped by adding 1-mL ethyl acetate, extracting the product twice. The empty vector enzyme was used

as negative control. The standard curves were plotted by authentic TIIA and iTIIA for quantification. K_m and k_{cat} were obtained by using GraphPad Prism version 5.0 (Motulsky, 2007), and the means \pm SE (standard error) were calculated from triplicates of assays.

The relative activities of SmTIIAS and its variants were assayed in vitro as described above. Mutants of SmTIIAS were generated by PCR using an overlap extension strategy with respective primers ([Supplemental Table S4](#)). The SmTIIAS mutant sequences were inserted into pET32a and the proteins were produced as described above.

Hairy root and RNAi

MeJA, SA, ABA, and GA were dissolved in dimethyl sulfoxide (DMSO) and applied to the hairy roots culture at the final concentrations of 50 μ M, 5 mM, 100 μ M, and 50 μ M, respectively, with addition of a DMSO solution (5%) as control. Hairy roots were harvested from the culture medium at 2 h after the treatments, then RNA was extracted. All treatments were performed in triplicate.

The region comprising nucleotides of 365–759 of SmTIIAS open reading frame was selected for double-stranded RNA generation. To target SmTIIAS precisely, this 395-bp fragment was compared with other 2-ODDs upregulated in *S. miltiorrhiza* root by blastn with cutoff of *e*-value $\leq 1e^{-10}$, which showed no substantial similarity. The fragment was cloned into gateway vector pDONR207, subsequently recombined into binary vector pK7GWIWG2R using a Gateway LR Clonase II enzyme mix (Invitrogen, Waltham, MA, USA). The disarmed *Agrobacterium tumefaciens* strain C58C1 containing pK7GWIWG2R-SmTIIAS was applied to infect aseptic *S. miltiorrhiza* leaf tissue (0.5 \times 0.5 cm) for 10 min, followed by transferring onto 6,7-V solid medium and co-cultured in the dark for 2 d, in presence of 400 mg/L carbenicillin to prevent *Agrobacterium* overgrowth. After 1 month, the hairy roots were transferred to liquid medium. The transgenic hairy roots were harvested for RNA isolation and metabolite extraction.

Quantitative reverse transcription PCR analysis

Hairy roots were collected and frozen in liquid nitrogen immediately, total RNA was isolated as described above and was reversed transcribed referring to the ReverTra Ace qPCR RT Kit (TOYOBO). RT-qPCR was performed with TB Green Premix Ex Taq (Takara, Shiga, Japan, RR420A). SmACTIN (Accession: HM231319) is used as internal reference gene, gene-specific primers as shown in [Supplemental Table S4](#), the relative expression of SmTIIAS was calculated following the formula of $2^{-\Delta\Delta Ct}$.

Metabolite extraction for UPLC and QE analysis

The plant tissues were dried by freeze dryer (Thermo), and 0.3 g each powder sample, was extracted with 5 mL of ethyl acetate, followed by ultrasonic crushing extraction for 1 h, drying ethyl acetate out by vacuum concentrator (Eppendorf, Hamburg, Germany), and dissolving in methanol for detection of metabolites. Chromatographic

separations were performed using the ACQUITY UPLC HSS C₁₈ column (2.1 × 100 mm, 1.8 μm, Waters) based on Agilent 1260 infinity II Prime LC system (Agilent, Santa Clara, CA, USA). A coupled Dionex UltiMate 3000 HPLC system and Q Exactive Plus Mass Spectrometer (Thermo Scientific) collected the MS (mass spectrum) data in positive-ion mode with the spray voltage 4 kV and capillary temperature 320°C, the stepped NCE (normalized collision energy) were set at 20, 40, and 70. Mobile phases with H₂O consisting of 0.1% formic acid (A) versus acetonitrile containing 0.1% formic acid (B) were used. The gradient profile was performed as following: 0 min, 50% A/50% B; 8 min, 20% A/80% B; 8.5 min, 0% A/100% B; 11 min, 0% A/100% B; 11.5 min, 50% A/50% B, which was held on for 3 min for re-equilibration, giving a total run time of 14.5 min. And the temperature of the column was maintained at 40°C. The flow rate of mobile phase is 0.5 mL/min with the 270 nm of detection wavelength.

Accession numbers

The sequences of *SmTIIAS*, *SbowTIIAS*, *SmeiTIIAS*, and *StriTIIAS* isolated in this work were verified by complete gene sequencing and have been submitted to the NCBI database with the accession numbers of MW916096, MW928604, MW928605, and MW928606, respectively. The transcriptome sequence data were deposited to NCBI Sequence Read Archive (SRA) with the accession number of PRJNA771193 and PRJNA771195.

Supplemental data

The following materials are available in the online version of this article.

Supplemental Figure S1. Aerial parts and roots of *S. miltiorrhiza* and *S. substolonifera*.

Supplemental Figure S2. UPLC profiles of enzyme activity of *SmTIIAS* *in vitro*.

Supplemental Figure S3. Effect of temperature and pH on enzyme activities of *SmTIIAS* using CT as substrate.

Supplemental Figure S4. Characterization of *SmTIIAS* activities by *in vitro* assay.

Supplemental Figure S5. The metabolites altered in accumulation in *SmTIIAS*-RNAi lines.

Supplemental Figure S6. The relative content of tanshinone IIA in *S. miltiorrhiza*, *S. meiliensis*, *S. bowleyana* and *S. trijuga*, respectively.

Supplemental Figure S7. Extended phylogenetic analysis of *TIIASs* and *Sm2-ODDs* with other experimentally characterized *2-ODDs*.

Supplemental Table S1. The annotation ratio statistics of *S. miltiorrhiza* and *S. substolonifera* transcriptome database.

Supplemental Table S2. The sequences of 18 *Sm2-ODD* candidate genes and the homologs from Xu and Song (2017).

Supplemental Table S3. Protein sequence information for the phylogenetic tree.

Supplemental Table S4. List of oligonucleotide primer sequences.

Acknowledgments

We thank Prof. Jian-Guo Cao (Shanghai Normal University) for supporting for this work. We also thank Dr Li-Jing Chang and Meng-Ying Cui for their generous help with this work.

Funding

This work was supported by the National Key R&D Program of China (Grant No. 2020YFA0907900), National Natural Science Foundation of China (Grant No. 32070338 and 31900255), the International Partnership Program of Chinese Academy of Sciences (153D31KYSB20160074), Strategic Biological Resources and Technology Supporting System from the Chinese Academy of Sciences (grant no. ZSZY-001), and the Special Fund for Shanghai Landscaping Administration Bureau Program (Grant No. G192419 and G222414).

Conflict of interest statement. The authors declare that there is no conflict of interest.

References

- Araujo WL, Martins AO, Fernie AR, Tohge T (2014) 2-Oxoglutarate: linking TCA cycle function with amino acid, glucosinolate, flavonoid, alkaloid, and gibberellin biosynthesis. *Front Plant Sci* 5: 552
- Beaudoin GAW, Facchini PJ (2014) Benzylisoquinoline alkaloid biosynthesis in opium poppy. *Planta* 240: 19–32
- Caarls L, Elberse J, Awwanah M, Ludwig NR, de Vries M, Zeilmaker T, Van Wees SCM, Schuurink RC, Van den Ackerveken G (2017) Arabidopsis JASMONATE-INDUCED OXYGENASES down-regulate plant immunity by hydroxylation and inactivation of the hormone jasmonic acid. *Proc Natl Acad Sci USA* 114: 6388–6393
- Cheng AX, Han XJ, Wu YF, Lou HX (2014) The function and catalysis of 2-oxoglutarate-dependent oxygenases involved in plant flavonoid biosynthesis. *Int J Mol Sci* 15: 1080–1095
- Dong Y, Morris-Natschke SL, Lee KH (2011) Biosynthesis, total syntheses, and antitumor activity of tanshinones and their analogs as potential therapeutic agents. *Nat Prod Rep* 28: 529–542
- Fang X, Li CY, Yang Y, Cui MY, Chen XY, Yang L (2017) Identification of a novel (-)-5-epieremophilene synthase from *Salvia miltiorrhiza* via transcriptome mining. *Front Plant Sci* 8: 627
- Fang ZY, Zhang M, Liu JN, Zhao X, Zhang YQ, Fang L (2021) Tanshinone IIA: a review of its anticancer effects. *Front Pharmacol* 11: 611087
- Farrow SC, Facchini PJ (2014) Functional diversity of 2-oxoglutarate/Fe(II)-dependent dioxygenases in plant metabolism. *Front Plant Sci* 5: 524
- Gao W, Hillwig ML, Huang L, Cui G, Wang X, Kong J, Yang B, Peters RJ (2009) A functional genomics approach to tanshinone biosynthesis provides stereochemical insights. *Organic Lett* 11: 5170–5173
- Ge C, Tang C, Zhu YX, Wang GF (2021) Genome-wide identification of the maize 2OGD superfamily genes and their response to *Fusarium verticillioides* and *Fusarium graminearum*. *Gene* 764: 145078
- Guo J, Ma X, Cai Y, Ma Y, Zhan Z, Zhou YJ, Liu W, Guan M, Yang J, Cui G, et al. (2016) Cytochrome P450 promiscuity leads to a

- bifurcating biosynthetic pathway for tanshinones. *New Phytol* **210**: 525–534
- Guo J, Zhou YJ, Hillwig ML, Shen Y, Yang L, Wang Y, Zhang X, Liu W, Peters RJ, Chen X, et al.** (2013) CYP76AH1 catalyzes turnover of miltiradiene in tanshinones biosynthesis and enables heterologous production of ferruginol in yeasts. *Proc Natl Acad Sci USA* **110**: 12108–12113
- Hansen BG, Kerwin RE, Ober JA, Lambrich VM, Mitchell-Olds T, Gershenzon J, Halkier BA, Kliebenstein DJ** (2008) A novel 2-oxoacid-dependent dioxygenase involved in the formation of the goiterogenic 2-hydroxybut-3-enyl glucosinolate and generalist insect resistance in *Arabidopsis*. *Plant Physiol* **148**: 2096–2108
- Hedden P, Thomas SG** (2012) Gibberellin biosynthesis and its regulation. *Biochem J* **444**: 11–25
- Hu GX, Takano A, Drew BT, Liu ED, Soltis DE, Soltis PS, Peng H, Xiang CL** (2018) Phylogeny and staminal evolution of *Salvia* (Lamiaceae, Nepetoideae) in East Asia. *Ann Bot* **122**: 649–668
- Huang JQ, Li DM, Tian X, Lin JL, Yang L, Xu JJ, Fang X** (2021) Side products of recombinant amorpho-4,11-diene synthase and their effect on microbial artemisinin production. *J Agric Food Chem* **69**: 2168–2178
- Islam MS, Leissing TM, Chowdhury R, Hopkinson RJ, Schofield CJ** (2018) 2-Oxoglutarate-dependent oxygenases. *Annu Rev Biochem* **87**: 585–620
- Johnson SR, Bhat WW, Bibik J, Turmo A, Hamberger B, Evolutionary Mint Genomics C, Hamberger B** (2019) A database-driven approach identifies additional diterpene synthase activities in the mint family (Lamiaceae). *J Biol Chem* **294**: 1349–1362
- Jonczyk R, Schmidt H, Osterrieder A, Fiesselmann A, Schullehner K, Haslbeck M, Sicker D, Hofmann D, Yalpani N, Simmons C, et al.** (2008) Elucidation of the final reactions of DIMBOA-glucoside biosynthesis in maize: characterization of Bx6 and Bx7. *Plant Physiol* **146**: 1053–1063
- Kakizaki T, Kitashiba H, Zou Z, Li F, Fukino N, Ohara T, Nishio T, Ishida M** (2017) A 2-oxoglutarate-dependent dioxygenase mediates the biosynthesis of glucoraphasatin in radish. *Plant Physiol* **173**: 1583–1593
- Kawai Y, Ono E, Mizutani M** (2014) Evolution and diversity of the 2-oxoglutarate-dependent dioxygenase superfamily in plants. *Plant J Cell Mol Biol* **78**: 328–343
- Ko WG, Kang TH, Lee SJ, Kim YC, Lee BH** (2001) Rotundifuran, a labdane type diterpene from *Vitex rotundifolia*, induces apoptosis in human myeloid leukaemia cells. *Phytother Res* **15**: 535–537
- Larbat R, Hehn A, Hans J, Schneider S, Jugde H, Schneider B, Matern U, Bourgaud F** (2009) Isolation and functional characterization of CYP71AJ4 encoding for the first P450 monooxygenase of angular furanocoumarin biosynthesis. *J Biol Chem* **284**: 4776–4785
- Larbat R, Kellner S, Specker S, Hehn A, Gontier E, Hans J, Bourgaud F, Matern U** (2007) Molecular cloning and functional characterization of psoralen synthase, the first committed monooxygenase of furanocoumarin biosynthesis. *J Biol Chem* **282**: 542–554
- Li DD, Ni R, Wang PP, Zhang XS, Wang PY, Zhu TT, Sun CJ, Liu CJ, Lou HX, Cheng AX** (2020a) Molecular basis for chemical evolution of flavones to flavonols and anthocyanins in land plants. *Plant Physiol* **184**: 1731–1743
- Li JT, Dong JE, Liang ZS, Shu ZM, Wan GW** (2008a) Distributional difference of fat-soluble compounds in the roots, stems and leaves of four *Salvia* plants. *Fen zi xi bao sheng wu xue bao. J Mol Cell Biol* **41**: 44–52
- Li MH, Chen JM, Peng Y, Wu Q, Xiao PG** (2008b) Investigation of Danshen and related medicinal plants in China. *J Ethnopharmacol* **120**: 419–426
- Li X, Luo D, Hou Y, Hou Y, Chen S, Zhan J, Luan J, Wang L, Lin D** (2020b) Sodium tanshinone IIA silate exerts microcirculation protective effects against spinal cord injury in vitro and in vivo. *Oxidat Med Cell Longev* **2020**: 3949575
- Ma Y, Cui G, Chen T, Ma X, Wang R, Jin B, Yang J, Kang L, Tang J, Lai C, et al.** (2021) Expansion within the CYP71D subfamily drives the heterocyclization of tanshinones synthesis in *Salvia miltiorrhiza*. *Nat Commun* **12**: 685
- Motulsky H** (2007) Prism 5 statistics guide, 2007. GraphPad Softw **31**: 39–42
- Murata J, Roepke J, Gordon H, De Luca V** (2008) The leaf epidermome of *Catharanthus roseus* reveals its biochemical specialization. *Plant Cell* **20**: 524–542
- Nakayasu M, Umemoto N, Ohyama K, Fujimoto Y, Lee HJ, Watanabe B, Muranaka T, Saito K, Sugimoto Y, Mizutani M** (2017) A dioxygenase catalyzes steroid 16 α -hydroxylation in steroidal glycoalkaloid biosynthesis. *Plant Physiol* **175**: 120–133
- Park YK, Obiang-Obounou BW, Lee J, Lee TY, Bae MA, Hwang KS, Lee KB, Choi JS, Jang BC** (2017) Anti-adipogenic effects on 3T3-L1 cells and Zebrafish by Tanshinone IIA. *Int J Mol Sci* **18**: 2065
- Pei T, Ma P, Ding K, Liu S, Jia Y, Ru M, Dong J, Liang Z** (2018) SmJAZ8 acts as a core repressor regulating JA-induced biosynthesis of salivianolic acids and tanshinones in *Salvia miltiorrhiza* hairy roots. *J Exp Bot* **69**: 1663–1678
- Sonawane PD, Heinig U, Panda S, Gilboa NS, Yona M, Kumar SP, Alkan N, Unger T, Bocobza S, Pliner M, et al.** (2018) Short-chain dehydrogenase/reductase governs steroidal specialized metabolites structural diversity and toxicity in the genus *Solanum*. *Proc Natl Acad Sci USA* **115**: E5419–E5428
- Tamura K, Stecher G, Peterson D, Filipinski A, Kumar S** (2013) MEGA6: molecular evolutionary genetics analysis version 6.0. *Mol Biol Evol* **30**: 2725–2729
- Tian X, Fang X, Huang JQ, Wang LJ, Mao YB, Chen XY** (2019) A gossypol biosynthetic intermediate disturbs plant defence response. *Philos Trans R Soc Lond B Biol Sci* **374**: 20180319
- Tian X, Ruan JX, Huang JQ, Yang CQ, Fang X, Chen ZW, Hong H, Wang LJ, Mao YB, Lu S, et al.** (2018) Characterization of gossypol biosynthetic pathway. *Proc Natl Acad Sci USA* **115**: E5410–E5418
- Turnbull JJ, Nakajima J, Welford RW, Yamazaki M, Saito K, Schofield CJ** (2004) Mechanistic studies on three 2-oxoglutarate-dependent oxygenases of flavonoid biosynthesis: anthocyanidin synthase, flavonol synthase, and flavanone 3 β -hydroxylase. *J Biol Chem* **279**: 1206–1216
- Vazquez-Flota F, De Carolis E, Alarco AM, De Luca V** (1997) Molecular cloning and characterization of desacetoxvindoline-4-hydroxylase, a 2-oxoglutarate dependent-dioxygenase involved in the biosynthesis of vindoline in *Catharanthus roseus* (L.) G. Don. *Plant Mol Biol* **34**: 935–948
- Viola G, Vedaldi D, dall'Acqua F, Basso G, Disaro S, Spinelli M, Cosimelli B, Boccacini M, Chimichi S** (2004) Synthesis, cytotoxicity, and apoptosis induction in human tumor cells by geiparvarin analogues. *Chem Biodivers* **1**: 1265–1280
- Wang L, Liu A, Zhang FL, Yeung JH, Li XQ, Cho CH** (2014) Evaluation and SAR analysis of the cytotoxicity of tanshinones in colon cancer cells. *Chin J Nat Med* **12**: 167–171
- Wang X, Morris-Natschke SL, Lee KH** (2007) New developments in the chemistry and biology of the bioactive constituents of Tanshen. *Med Res Rev* **27**: 133–148
- Xu Z, Song J** (2017) The 2-oxoglutarate-dependent dioxygenase superfamily participates in tanshinone production in *Salvia miltiorrhiza*. *J Exp Bot* **68**: 2299–2308
- Yang L, Ding G, Lin H, Cheng H, Kong Y, Wei Y, Fang X, Liu R, Wang L, Chen X, et al.** (2013) Transcriptome analysis of medicinal plant *Salvia miltiorrhiza* and identification of genes related to tanshinone biosynthesis. *PLoS One* **8**: e80464
- Zhang Z, Zhang J, Jin L, Song T, Wu G, Gao J** (2008) Tanshinone IIA interacts with DNA by minor groove-binding. *Biol Pharm Bull* **31**: 2342–2345